

## Magnetic-field-induced phase transition in BiFeO<sub>3</sub> observed by high-field electron spin resonance: Cycloidal to homogeneous spin order

Benjamin Ruetter,<sup>1</sup> S. Zvyagin,<sup>2</sup> A. P. Pyatakov,<sup>3</sup> A. Bush,<sup>4</sup> J. F. Li,<sup>1</sup> V. I. Belotelov,<sup>3</sup> A. K. Zvezdin,<sup>3</sup> and D. Viehland<sup>1</sup>

<sup>1</sup>Department of Materials Science and Engineering, Virginia Tech, Blacksburg, Virginia 24061, USA

<sup>2</sup>The National High Magnetic Field Laboratory, 1800 E. Paul Dirac Drive, Tallahassee, Florida 32310, USA

<sup>3</sup>Institute of General Physics, Russian Academy of Science, Vavilova St., 38, Moscow 119991, Russia

<sup>4</sup>Moscow State Institute of Radio Engineering, Electronics and Automation (Technical University), Vernadskii Prospect, 78, Moscow 117454, Russia

(Received 24 April 2003; revised manuscript received 29 September 2003; published 27 February 2004)

Bismuth ferrite is a magnetoelectric material, which simultaneously has polarization and spin orders. We have used electron spin resonance (ESR) as a local probe of the magnetic order in the magnetic-field range of 0–25 T, in the frequency domain of 115–360 GHz, and at a temperature of 4.2 K. The data reveal significant changes in the ESR spectra with increasing field, which have been analyzed by taking into account the magnetic anisotropy of the crystal and a magnetoelectric Dzyaloshinsky-Moria-like interaction. The results demonstrate an induced phase transition from an incommensurately cycloidal modulated state to one with homogeneous spin order.

DOI: 10.1103/PhysRevB.69.064114

PACS number(s): 77.80.-e, 75.25.+z, 75.80.+q

### I. INTRODUCTION

Multiferroic materials have two order parameters. They can be spontaneous polarization (ferroelectric or antiferroelectric) and a spontaneous magnetization (ferromagnetic or antiferromagnetic).<sup>1</sup> The magnetoelectric effect is the coupling between the spontaneous polarization  $P_s$  and the spontaneous magnetization  $M_s$ . Phenomenologically, this coupling can be either mediated by linear, biquadratic, or even higher-order exchanges.<sup>2</sup>

One of the first multiferroic materials found was BiFeO<sub>3</sub>,<sup>3</sup> which has a perovskitelike structure. It has been demonstrated that BiFeO<sub>3</sub> has two order parameters:<sup>1</sup> (i) a polarization (ferroelectric) ordering with a high Curie temperature  $T_C$  of 1103 K;<sup>3,4</sup> and (ii) a spin (antiferromagnetic) ordering of the  $G$  type with a magnetic transition temperature  $T_N$  of 643 K.<sup>5–7</sup> Clearly, the spin and polarization orderings are driven by different modes, as the phase-transition temperatures are significantly different.

The average crystal lattice of BiFeO<sub>3</sub> is a rhombohedrally distorted perovskite structure,<sup>5,7–12</sup> which belongs to the space group  $R3c$  (or  $C_6^{3V}$ ), as shown in Fig. 1(a). The hexagonal unit-cell parameters are  $a = 5.58 \text{ \AA}$  and  $c = 13.9 \text{ \AA}$ . In this structure, along the threefold pseudocubic  $[111]_c$  rotation axis, the Bi<sup>3+</sup> and Fe<sup>3+</sup> cations are displaced from their centrosymmetric positions. This centrosymmetric distortion is polar, and results in a spontaneous polarization ( $P_s$ ), as illustrated in Fig. 1(a). Previous investigations of the polarization behavior of oriented single crystals have shown a  $P_s$  of 0.035 C/m<sup>2</sup> along the  $[001]_c$  at 77 K.<sup>10</sup> However, recent investigations of single crystalline thin layers fabricated by pulsed laser deposition have shown a much higher  $P_s$  along the  $[001]_c$  and  $[111]_c$ , approaching values of 0.6 C/m<sup>2</sup> (Ref. 13) and 1 C/m<sup>2</sup> (Ref. 14) at room temperature, respectively.

Antiferromagnetic ( $T_N \sim 643 \text{ K}$ ) BiFeO<sub>3</sub> has weak magnetism at room temperature.<sup>1</sup> The spin is provided by the transition-metal cation Fe<sup>3+</sup>. Spins in the neighboring atoms

are antiparallel, leading to an antiferromagnetic ordering of the  $G$  type.<sup>1,7</sup> In this arrangement, the Fe<sup>3+</sup> cations are surrounded by six nearest Fe<sup>3+</sup> neighbors, with opposite spin directions. Figure 1(b) shows the hexagonal representation of the spin structure of BiFeO<sub>3</sub>. In this structure, the hexagonal  $[001]_h$  direction is equivalent to the pseudocubic  $[111]_c$ , about which axis there is a threefold rotation; and about the hexagonal  $[110]_h$ , there is a mirror plane. Thus along the  $[001]_h/[111]_c$ , BiFeO<sub>3</sub> has antiferromagnetic order, as illustrated in Fig. 1(b).

Microscopically, the antiferromagnetic spin order is not homogeneous for BiFeO<sub>3</sub> single crystals. Precise neutron-diffraction studies<sup>15,16</sup> have revealed an incommensurately modulated spin structure which manifests itself as a cycloid with a long wavelength  $\lambda$  of  $\sim 600 \text{ \AA}$ . In the incommensurate phase, the periodicity of the spin polarization is incommensurate with the crystallographic lattice parameters. The cycloidal spin structure has been shown to be directed along  $[110]_h$ . The existence of the incommensurate cycloid has also been confirmed by line-shape analysis of nuclear magnetic resonance (NMR) spectra.<sup>17,18</sup> In BiFeO<sub>3</sub>, the spin profile is nearly sinusoidal and the phase of the modulation is a linear function of the space coordinate in the direction of the modulation.<sup>15,19</sup> However, temperature-dependent NMR studies have revealed that the spin profile becomes increasingly anharmonic as the temperature is decreased.<sup>17</sup> Similar phenomena are observed in dielectrics where spatial profiles of polarization can be strongly anharmonic near the temperature of phase transition to a commensurate polar state, which consists of nearly commensurate regions separated by domain walls (i.e., solitons) where the phase of the order parameter changes abruptly. In addition, the spin profile of BiFeO<sub>3</sub> becomes anharmonic with increasing magnetic field  $H$ . At higher fields of  $H > 18 \text{ T}$ , an induced phased transition has been reported.<sup>20–22</sup> Previously, in other materials, changes in the spatial profile of incommensurate structures,<sup>23–25</sup> in soliton density,<sup>23,26,27</sup> and soliton dimensionality ( $1-q$  vs  $3-q$ ) (Refs. 28 and 29) with increasing magnetic and/or electric field have been reported.

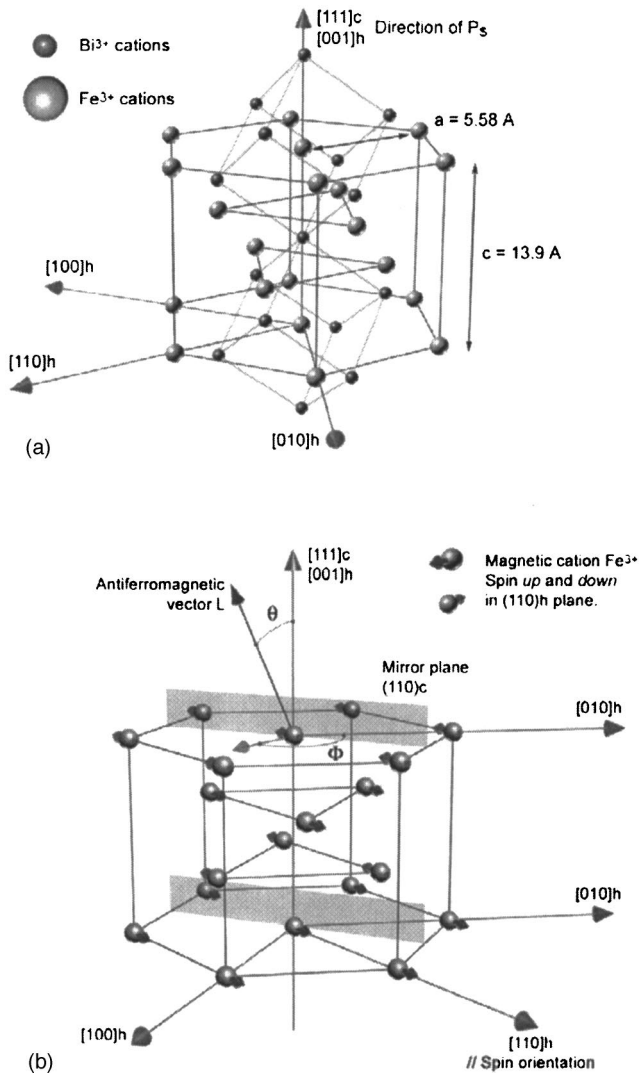


FIG. 1. (a) Crystal lattice of BiFeO<sub>3</sub>, illustrating rhombohedral units and hexagonal cell. The direction of spontaneous polarization is illustrated in this figure. (b) Hexagonal representation of spin structure of BiFeO<sub>3</sub>. Both the antiferromagnetic order and spin rotation planes are shown in this figure.

The intrinsic spin-phonon coupling is generally small,<sup>1</sup> as it involves a relativistic interaction between the two order parameters  $P_s$  and  $M_s$ . Phenomenologically, the linear exchange between the two in the Landau-Ginzburg equation of state, i.e.,  $P_i = Q_{ij}M_j$ , inherently involves a coupling between the linear power of a polar tensor and a linear power of an axial tensor.<sup>30–37</sup> This intrinsic linear coupling coefficient  $Q_{ij}$  does not have a normal symmetric tensor matrix as a solution. Rather, the linear magnetoelectric exchange must have an antisymmetric component in its property tensor,<sup>30–37</sup> in addition to the usual symmetric one.

In BiFeO<sub>3</sub>, the conventional Dzyaloshinsky-Moria interaction is zero. It is forbidden by the space-group symmetry. A linear magnetoelectric Dzyaloshinsky-Moria-like interaction is allowed by the  $3m$  magnetic point group.<sup>34</sup> Nevertheless, polarization measurements have shown that it is not observed in BiFeO<sub>3</sub> when the cycloidal spin structure is present.<sup>20–22</sup> The magnetoelectric effect is averaged to zero

due to the fact that the average value of the projection of the antiferromagnetic vector in the cycloidal structure is zero. However, the cycloidal structure does not prevent manifestation of the quadratic magnetoelectric effect.<sup>38</sup>

The spin cycloidal structure that prevents the linear magnetoelectric effect from being observed can be destroyed by high magnetic field. Application of high magnetic field can induce a phase transition from a spatially modulated spin structure to one with a homogeneous spin order. Previously, an induced phase transition and the appearance of a linear magnetoelectric effect have been reported by polarization measurements under a pulse magnetic field of 20 T.<sup>20–22</sup>

Electron spin resonance (ESR) has been shown to be a very powerful tool for the study of magnetic excitation and phase transitions in solids.<sup>39,40</sup> The main purpose of this investigation was to study the magnetic excitation spectrum of BiFeO<sub>3</sub> crystals over a broad frequency range under steady magnetic fields up to 25 T. It was anticipated that this investigation would provide a more thorough and reliable understanding of magnetic-field-induced phase transitions and magnetoelectric coupling at high magnetic fields in BiFeO<sub>3</sub>.

## II. EXPERIMENTAL PROCEDURE

Bismuth ferrite single crystals were grown by a flux method from a Bi<sub>2</sub>O<sub>3</sub>-Fe<sub>2</sub>O<sub>3</sub>-NaCl melt. Single crystals were oriented along the [001]<sub>c</sub>. Specimens were cut into dimensions of 1 × 1 × 0.5 mm<sup>3</sup>. The structure was rhombohedral (or hexagonal) and the crystal lattice parameters were  $a = b = c = 5.61 \text{ \AA}$  and  $\alpha = 89.28^\circ$  (or  $a = 5.58 \text{ \AA}$  and  $c = 13.9 \text{ \AA}$ ).

ESR is an extremely powerful tool to test magnetic excitation spectra in solids, providing important information on a magnetic structure and main parameters of the effective spin Hamiltonian. In order to test the field-induced phase transition in BiFeO<sub>3</sub>, high-field ESR measurements were performed using the submillimeter facility at the National High Magnetic Field Laboratory (NHMFL, Tallahassee, FL), in fields up to 25 T. Investigations have been done in the frequency range of 115–360 GHz. Quasicontinuously retuned sources of millimeter and submillimeter wave radiation, backward wave oscillators, were used. Transmission-type ESR spectrometer with oversized cylindrical waveguides and a sample holder in the Faraday configuration (with a wave propagation vector parallel to the external field) was employed. A high-homogeneity (12 ppm/cm DSV) magnetic field was produced by the 25-T hysteresis-free resistive Bitter-type W. M. Keck magnet. In our experiment, the magnetic field was oriented along the pseudocubic [001]<sub>c</sub> direction. Since absorption lines were relatively broad, an optical modulation of the microwave power was used. The spectra were recorded during the magnetic field sweeping. A low noise, wide frequency range, InSb hot electron bolometer, operated at liquid-He temperatures served as a detector. Experiments were performed at a temperature of 4.2 K.

## III. ESR SPECTRA

Figure 2 shows the ESR signal as a function of magnetic field for  $0 < H < 25 \text{ T}$ , taken at various frequencies between

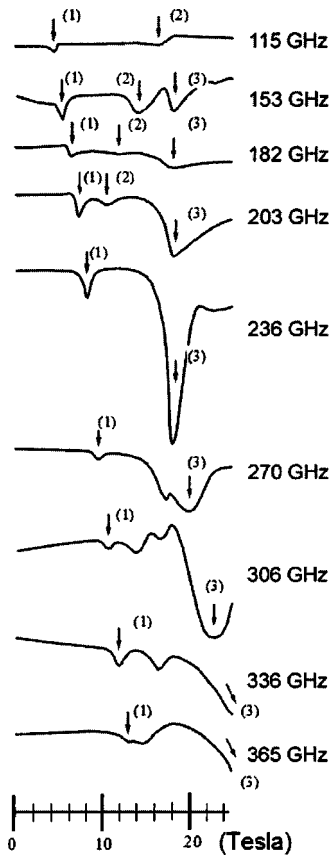


FIG. 2. ESR spectra for  $\text{BiFeO}_3$  at  $T=4.2$  K as a function of magnetic field between 0 and 25 T for various submillimeter frequencies between 115 and 365 GHz. The symbols (1), (2), and (3) represent different absorption peaks: they are illustrated to guide the eyes with their shift with frequency.

$115 < \nu < 360$  GHz. This figure shows dramatic changes in the ESR spectra for the various frequencies. At lower frequencies  $\nu > 115$  GHz, a single absorption peak was found at lower magnetic fields, as illustrated by an arrow (1). With increasing  $\nu$ , this absorption peak was continuously shifted to higher fields ( $\nu \sim H$ ) and the degree of absorption was increased, as illustrated by arrows labeled as (1). Additional peaks were found in higher fields, denoted by arrows labeled as (2) and (3).

Of particular interest was the peak indicated by arrows labeled as (3) in Fig. 2, which became apparent for  $\nu > 200$  GHz. This resonance absorption was quite pronounced, and in fact the attenuation of the submillimeter radiation in the crystal at this resonance was significant. With increasing  $\nu$ , this peak continuously shifted to higher  $H$  ( $\nu \sim H$ ), the adsorption became increasingly pronounced, and the peak became increasingly broad. Clearly, under high magnetic field, a secondary resonance state is induced. The shape of this secondary resonance peak is noticeably dependent upon  $H$  and  $\nu$ .

#### Resonance frequency vs $H$

The experimental observations of the dependence of the resonance frequencies  $\nu$  on  $H$  are summarized in Fig. 3.

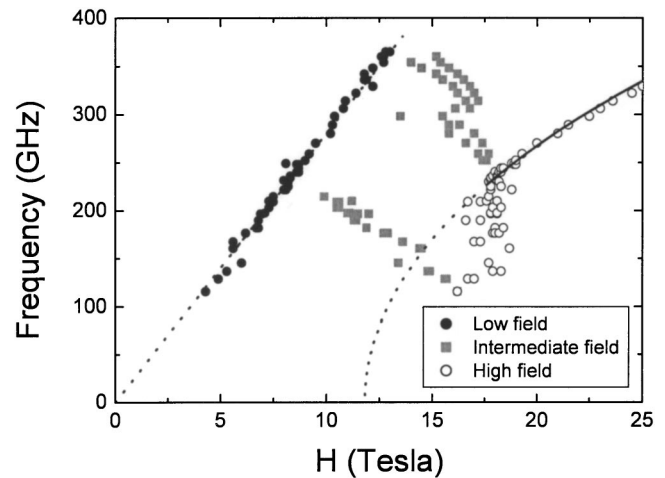


FIG. 3. Electron spin resonance frequency as a function of magnetic field  $H$  ( $T=4.2$  K).

The maximum of the absorption has been chosen to indicate the resonance field. Clearly, there is more than one resonance mode present over the magnetic field range investigated.

#### 1. Low ( $0 < H < 10$ T)-field range

A low-field spin-resonance mode was observed that had a linear relationship between  $\nu$  and  $H$ , which had a slope of  $\sim 27$  GHz/T (that corresponds to Lande  $g$  factor of  $\sim 2.0$ ) and a slope intercept of zero. These data are illustrated in Fig. 3 using closed circle symbols and dashed line. This is the spin-resonance mode that corresponds to the arrows labeled as (1) in Fig. 2.

The cycloidal modulation has previously been measured by temperature-dependent NMR studies,<sup>17,18</sup> but ESR studies are without precedent. The NMR studies revealed that the spin profile is anharmonic at 4.2 K, becoming increasingly sinusoidal with increasing temperature.<sup>17</sup>

#### 2. Intermediate ( $10 < H < 18$ T)-field range

The low-field spin mode was found to continue until higher fields, maintaining the same slope value of  $g \sim 2$ . However, an “intermediate-field range” of  $10 < H < 18$  T can be designated, based upon the presence of an additional resonance peak whose resonance frequency decreased with increasing  $H$ , as shown in Fig. 3 by the gray square symbols. This is an anomalous result as both the  $g$  factor and magnetic permeability are positive.

In addition, hysteretic effects became very pronounced between ESR spectra obtained on increasing vs decreasing  $H$  sweeps. This is further illustrated in Fig. 4, which shows a representative ESR signal taken at a measurement frequency of 236 GHz. In this figure, significant hysteretic effects were found in the intermediate field range of  $10 < H < 18$  T. Hysteresis effects are known in pinned incommensurate structures, see, for instance, in the field-induced incommensurate phase of  $\text{CuGeO}_3$ .<sup>41,42</sup>

The data support a model of an incommensurately modulated cycloidal structure whose spin profile is changed

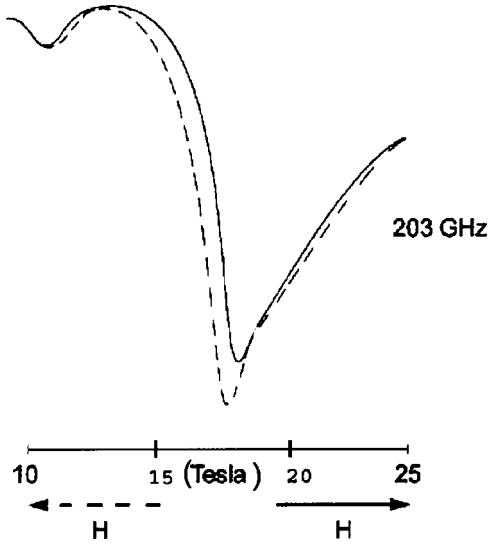


FIG. 4. Representative ESR signal illustrating hysteretic effects present in the intermediate field range of  $10 < \vec{H} < 18$  T. The closed line was taken on increasing field sweep, and the dashed line was taken on decreasing field sweep.

by application of  $H$ . The spiral structure becomes increasingly anharmonic with increasing  $H$  as an induced phase transition is approached. In addition, the spin cycloid may become depinned with increasing  $H$ , resulting in hysteretic effects.

### 3. High-field range of $H > 18$ T

Figure 3 clearly demonstrates an induced phase transition near  $H = 18$  T. In the high-field range, a secondary spin-resonance mode was observed. These data are shown as open circles in Fig. 3. The slope of this secondary spin mode was  $\sim \frac{1}{2}$  of that of the low-field one, having a value of 13 GHz/T. No hysteretic effects were observed in the ESR spectra, within this secondary mode.

It is important to notice that the primary (low-field) spin mode can be linearly extrapolated into the high-field regime, revealing the presence of a field-induced gap state. Due to strong microwave absorption at higher frequencies, it was found difficult to experimentally confirm the linear extrapolation. However, the ESR spectra at 365 GHz clearly show this primary resonance persisting, which was of noticeable absorption. The data indicate an induced gap for  $H > 18$  T.

To understand the nature of the secondary resonance mode, it is thus necessary to develop a theoretical approach. We conjecture that the induced phase transformation is from the cycloidal to a homogeneously magnetized state. In the following section, we shall present this theoretical formulation, and show supporting evidence.

## IV. LANDAU-GINZBURG THEORY FOR FIELD-INDUCED TRANSITION, AND ESR SPECTRA

In this section, a Landau-Ginzburg (LG) formalism for the free energy will be considered. A theory for the field-induced

phase transition of  $\text{BiFeO}_3$  and changes in the ESR spectra will then be given. The Landau-Ginzburg energy<sup>19</sup> of the spin structure of  $\text{BiFeO}_3$  is the sum

$$F = F_L + F_{exch} + F_{an} + F_m, \quad (1)$$

where  $F_L$  is the magnetoelectric coupling that is linear in gradient, in which the Lifshitz invariant is responsible for the creation of the spatially modulated spin structure,  $F_{exch}$  is the inhomogeneous exchange energy,  $F_{an}$  is the anisotropy energy, and  $F_m$  is the magnetic energy.

We have formulated a solution to the LG equation,<sup>43–45</sup> whose derivation can be found in the EPAPS system.<sup>46</sup> The volume-averaged free energy of the spin cycloid state ( $F_{\text{cycloid}}$ ), under a magnetic field parallel to the  $[001]_c$  direction of  $H = (H_x, 0, H_z)$ , is

$$F_{\text{cycloid}} = -\chi_{\perp} \frac{H^2}{2} - \frac{1}{4A} (\alpha \cdot P_z)^2 + \frac{K_u}{2} + \frac{5}{8} K_2 - \chi_{\perp} \frac{(\beta \cdot P_z)^2}{4} + \chi_{\perp} \frac{H_z^2}{4}, \quad (2)$$

where  $\chi_{\perp}$  is the magnetic susceptibility of the media in the direction perpendicular to the antiferromagnetic vector  $\vec{l}$ ,  $A$  is a stiffness coefficient,  $\alpha$  is the inhomogeneous relativistic exchange constant (inhomogeneous magnetoelectric constant),  $P_z$  is spontaneous polarization,  $K_u$  is the uniaxial magnetic anisotropy constant,  $K_2$  is the second-order anisotropy, and  $\beta$  is the homogeneous magnetoelectric constant (i.e., a magnetoelectriclike Dzyaloshinsky-Moria, or DM, interaction). A phase transition to the homogeneous antiferromagnetic spin state will occur at a critical field  $H_c$ , when the energy of the homogeneous state is equal to that one of the cycloidal one. The energy of the homogeneous antiferromagnetic state ( $F_{\text{homogenous}}$ ), under an external field of  $H = (H_x, 0, H_z)$ , is

$$F_{\text{homogenous}} = -\frac{\chi_{\perp} \cdot H^2}{2} + K_u + K_2 - \chi_{\perp} \frac{(\beta \cdot P_z)^2}{2} - \chi_{\perp} (\beta \cdot P_z) H_x. \quad (3)$$

The dynamic properties of the cycloidal spin modulated and of the induced homogeneous antiferromagnetic spin states can be predicted by a Lagrangian method; again see EPAPS system for details.<sup>46</sup> The ESR resonance frequency  $\nu$  for fields of  $H > H_c$  is

$$\nu = \frac{\omega}{2\pi} = \frac{\gamma}{2\pi} \sqrt{\left( \frac{-b \pm \sqrt{b^2 - 4c}}{2} \right)}, \quad (4a)$$

$$b = \frac{2K_u}{\chi_{\perp}} - H_z^2 - (\beta \cdot P_z)^2 - 2(\beta \cdot P_z) H_x - H_x^2, \quad (4b)$$

$$c = \left( \frac{2K_u}{\chi_{\perp}} - (\beta \cdot P_z)^2 - H_z^2 - (\beta \cdot P_z) H_x \right) (-H_x^2 - (\beta \cdot P_z) H_x) - (H_x H_z)^2, \quad (4c)$$

where  $\gamma = 1.73 \times 10^7 \sqrt{\text{cm/g}}$  is the gyromagnetic ratio.



### Predictions and supporting evidence

Equations (4a)–(4c) describe the magnetic-field dependence of the electron spin resonance frequency for a homogeneous spin state. It is not applicable to the cycloidal spin state, as the gradient terms were excluded; see EPAPS system.<sup>46</sup> Equations (4a)–(4c) demonstrate that the resonant frequency of the homogeneous spin phase is dependent only upon two independent parameters:

- (i) an anisotropic magnetic factor, given as

$$\frac{K_u}{\chi_\perp}, \text{ and} \quad (5a)$$

- (ii) a polarization factor that is coupled to the magnetization  $m$  through the linear magnetoelectric coefficient  $\beta$  of the homogenous spin ordered state, given as

$$H_{DM} = \beta \cdot P_z = \frac{m}{\chi_\perp}, \quad (5b)$$

where  $H_{DM}$  is the Dzyaloshinsky-Moria field. In the homogeneous spin state, there will be a net magnetoelectric effect that is equal to  $\beta$ .

These two parameters can be obtained by fitting to the experimental data. Figure 3 shows the result of this fitting, illustrated as dashed lines. It yields values for the anisotropic magnetic factor of  $K_u/\chi_\perp = 1.41 \times 10^{10}$  erg/cm<sup>3</sup>, and for the Dzyaloshinsky-Moria field of  $D = \beta \cdot P_z = 1.19 \times 10^5$  Oe (or 11.9 T). The dashed curve, corresponding to the solution involving  $-\sqrt{b^2 - 4c}$  in Eq. (4a), is in good agreement with the experimental data for fields above that of the induced phase transition ( $\sim 18$  T). Near, but below this field, there was an apparent noise in the data, due to hysteresis around the phase-transition point. Our solution cannot account for this hysteresis, as it does not apply for  $H < H_c$ . The solution involving  $+\sqrt{b^2 - 4c}$  in Eq. (4a) gives frequencies much greater than that of the upper limit of our experimental range, and thus has not been experimentally verified.

The uniaxial anisotropy constant  $K_u$  can also be calculated from the ESR data. Using the reported value<sup>47</sup> for the perpendicular susceptibility of  $\chi_\perp = 4.7 \times 10^{-5}$ , the uniaxial anisotropy constant can be approximated as  $K_u = 6.6 \times 10^5$  erg/cm<sup>3</sup>. Using values of  $H_c = 1.8 \times 10^5$  Oe,  $A \approx 8 \times 10^{-7}$  erg/cm (estimated from NMR data<sup>17</sup>),  $\alpha \cdot P_z = 2Aq$ ,  $q = 2\pi/\lambda$ , and  $\lambda = 620$  Å,<sup>15</sup> the value of the second-order anisotropy constant can be approximated as  $K_2 \sim 10^4$  erg/cm<sup>2</sup>.

The agreement of the theory and the high-field electron spin resonance mode demonstrates that the induced phase is the homogeneous antiferromagnetic spin state. The cycloidal spin structure is destroyed by increasing magnetic field, resulting in homogeneous spin order. The term homogeneous does not designate a single-crystal, single domain state which has homogenous order through out the specimen; such a condition only requires the Lifshitz invariant term to be zero in the free-energy expansion. Rather, we use the term homogeneous to designate that the local pattern of spin arrangement is uniform within the domains. Accordingly, the spatial profile is uniform (cycloidal structure de-

stroyed), and the magnetoelectric coefficients are not averaged to zero.

## V. DISCUSSION AND SUMMARY

Bismuth ferrite at low fields has a cycloidal spin structure.<sup>15–19</sup> The cycloidal structure is periodically modulated with  $\lambda \sim 600$  Å. The spin profile is slightly anharmonic. To condense the homogeneously magnetized state requires the field-forced destruction of the long-wavelength cycloidal modulation. We have performed investigations of the electron spin resonance modes of BiFeO<sub>3</sub> as a function of magnetic field. Studies were done up to very high magnetic fields (25 T), sufficient to force the spin alignment, and to condense a homogeneous spin order.

We summarize the observed changes in spin structure as follows. At low to moderate fields, a cycloidal spin structure exists. The profile and modulation wavelength of the cycloidal structure are changed with  $H$ . With increasing  $H$ , the incommensurate structure becomes depinned, resulting in hysteretic effects between increasing and decreasing  $H$  sweeps. Above some critical field  $H_c$ , a transition to a homogeneously magnetized state is induced. This transition results in the destruction of the spin cycloid. Phenomenologically, the order parameter of the transition between the cycloidal and homogeneously magnetized states is dependent on the inhomogeneous and homogeneous magnetoelectric coefficients ( $\alpha$  and  $\beta$ , respectively).

The ESR peaks in the homogeneous magnetized state were found to be quite broad, and in fact became increasingly broad with increasing  $H$  for  $H > H_c$ , as can be seen in Fig. 2. Peak broadening of ESR and NMR spectra has previously been described using a multisoliton theory.<sup>23,25–29</sup> Our results indicate that there may be numerous regions of homogeneously magnetized spin order.

### A. Comparison of our estimated value for $\beta$ with that recently reported for BiFeO<sub>3</sub> thin layers

Recent investigations of (001)-oriented BiFeO<sub>3</sub> epitaxial thin layers grown on strontium titanate have shown dramatically higher values of the spontaneous ( $P_s$ ) and remanent ( $P_r$ ) polarizations<sup>13</sup> than for bulk single crystals. The saturation polarization of the thin layer can be seen to be  $\sim 0.52$  C/m<sup>2</sup>, which is much higher than the value of  $0.035$  C/m<sup>2</sup> previously reported for (001)-oriented single crystals. In addition, the (001)-oriented BiFeO<sub>3</sub> thin layers were reported to have dramatically higher magnetoelectric (ME) coefficients,<sup>13</sup> than the bulk crystals. The value of the ME coefficient of the thin layers in the remanently polarized and magnetized states is  $\sim 3.5$  V/Oe cm.

The significant changes in the magnetoelectric, ferroelectric, and ferromagnetic behavior of the thin layers might be understood in terms of an epitaxially induced homogeneously magnetized state. To support this possibility, we estimated the value of the magnetoelectric coefficient of the homogeneous spin state for the single crystal of

BiFeO<sub>3</sub> from the measured value of  $H_{DM}$ , comparing it to the reported value of the magnetoelectric coefficient of (001)-oriented BiFeO<sub>3</sub> thin layers. Rearrangement of Eq. (5b) gives the homogeneous ME coefficient  $1/\beta$  in units of V/Oe m,

$$\frac{1}{\beta_3} \left[ \frac{\text{V}}{\text{Oe m}} \right] = \frac{P_z}{\epsilon_o K H_{DM}}, \quad (6a)$$

where  $\epsilon_o$  is the permittivity of free space and  $K$  is the relative dielectric constant which is equal to  $\sim 100$ .<sup>13</sup> The value of  $1/\beta_3$  can be estimated from the measured value of  $H_{DM} = 1.2 \times 10^5$  Oe in Fig. 3, and the inherent value of  $P_z = 0.035$  C/m<sup>2</sup> of the single crystal.<sup>10</sup> The value of  $1/\beta_3$  for the homogeneously spin ordered state is

$$\frac{1}{\beta_3} = \frac{0.035}{8.85 \times 10^{-12} \times 100 \times 1.2 \times 10^5} \left[ \frac{\text{V}}{\text{Oe m}} \right] = 3.3 \left[ \frac{\text{V}}{\text{Oe cm}} \right]. \quad (6b)$$

Comparisons of the predicted value of  $1/\beta_3$  in Eq. (6b) with the experimentally observed value in Ref. 13 of 3.5 V/Oe cm will demonstrate remarkable agreement. This indicates that a homogeneous spin state might be induced by either application of high magnetic field or by epitaxial constraint (or alternatively by the influence of boundary conditions), suggesting the possibility to release the latent magnetoelectricity locked within the cycloid.

## B. Summary

In this investigation, we have reported experimental evidence of a high magnetic-field-induced phase transformation between a cycloidal and a homogeneous magnetized state in BiFeO<sub>3</sub>. The field dependence of electron spin resonance modes have been theoretically predicted using Landau-Ginzburg theory that includes a relativistic antisymmetric exchange, and experimentally confirmed by high-field ESR measurements. The transformation between cycloidal and homogeneous spin orders is related to a Lifshitz invariant in the free-energy expansion that is magnetoelectric in nature. In both states, the magnetoelectric coefficient  $\beta$  is the same, but the ME coefficient is only manifested in the homogeneous one.

## ACKNOWLEDGMENTS

We gratefully acknowledge the support of the Office of Naval Research under Grant Nos. N000140210340, N000140210126, and MURI N000140110761, and to RFBR 01-02-1695. A portion of this work was performed at the National High Magnetic Field Laboratory, which is supported by NSF Cooperative Agreement No. DMR-0084173 and by the State of Florida.

- 
- <sup>1</sup>G. A. Smolenskii and I. Chupis, *Sov. Phys. Usp.* **25**, 475 (1982).  
<sup>2</sup>D. K. H. Salje, *Phase Transitions in Ferroelastic and Co-elastic Crystals* (Cambridge University Press, Cambridge, 1990).  
<sup>3</sup>Yu. N. Venetsev, G. Zhdanov, and S. Solov'ev, *Sov. Phys. Crystallogr.* **4**, 538 (1960).  
<sup>4</sup>G. Smolenskii, V. Isupov, A. Agranovskaya, and N. Krainik, *Sov. Phys. Solid State* **2**, 2651 (1961).  
<sup>5</sup>P. Fischer, M. Polomskya, I. Sosnowska, and M. Szymanski, *J. Phys. C* **13**, 1931 (1980).  
<sup>6</sup>G. Smolenskii, V. Yudin, E. Sher, and Yu. E. Stolypin, *Sov. Phys. JETP* **16**, 622 (1963).  
<sup>7</sup>S. Kiselev, R. Ozerov, and G. Zhdanov, *Sov. Phys. Dokl.* **7**, 742 (1963).  
<sup>8</sup>C. Michel, J-M. Moreau, G. D. Achenbach, R. Gerson, and W. J. James, *Solid State Commun.* **7**, 701 (1969).  
<sup>9</sup>J. D. Bucci, B. K. Robertson, and W. J. James, *J. Appl. Crystallogr.* **5**, 187 (1972).  
<sup>10</sup>J. R. Teague, R. Gerson, and W. J. James, *Solid State Commun.* **8**, 1073 (1970).  
<sup>11</sup>Yu. E. Roginskaya, Yu. Ya. Tomashpol'skii, Yu. N. Venetsev, V. M. Petrov, and G. S. Zhdanov, *Sov. Phys. JETP* **23**, 47 (1966).  
<sup>12</sup>F. Kubel and H. Schmid, *Acta Crystallogr., Sect. B: Struct. Sci.* **B46**, 698 (1990).  
<sup>13</sup>J. Wang, H. Zheng, V. Nagarajan, B. Liu, S. B. Ogale, D. Viehland, V. Venugopalan, D. G. Schlom, M. Wuttig, R. Ramesh, J. B. Neaton, U. V. Waghmare, N. A. Hill, and K. M. Rabe, *Science* **299**, 1719 (2003).  
<sup>14</sup>J. Wang, B. Ruetter, M. Wuttig, R. Ramesh, and D. Viehland (unpublished).  
<sup>15</sup>I. Sosnowska, T. Peterlin-Neumaier, and E. Steichele, *J. Phys. C* **15**, 4835 (1982).  
<sup>16</sup>I. Sosnowska, M. Loewenhaupt, W. I. F. David, and R. Ibberson, *Physica B* **180&181**, 117 (1992).  
<sup>17</sup>A. Zaleskii, A. Zvezdin, A. Frolov, and A. Bush, *JETP Lett.* **71**, 465 (2000).  
<sup>18</sup>A. V. Zaleskii, A. A. Frolov, T. A. Khimich, A. A. Bush, V. S. Pokatilov, and A. K. Zvezdin, *Europhys. Lett.* **50**, 547 (2000).  
<sup>19</sup>I. Sosnowska and A. Zvezdin, *J. Magn. Magn. Mater.* **140-144**, 167 (1995).  
<sup>20</sup>Yu. F. Popov, A. Zvezdin, G. Vorob'ev, A. Kadomtseva, V. Murashev, and D. Rakov, *JETP Lett.* **57**, 69 (1993).  
<sup>21</sup>A. Kadomtseva, Yu. Popov, G. Vorob'ev, and A. Zvezdin, *Physica B* **211**, 327 (1995).  
<sup>22</sup>Yu. F. Popov, A. Kadomtseva, S. Krotov, D. Belov, G. Vorob'ev, P. Makhov, and A. Zvezdin, *Low Temp. Phys.* **27**, 478 (2001).  
<sup>23</sup>R. Blinc and A. P. Levanyuk, *Incommensurate Phases in Dielectrics* (North-Holland, New York, 1986).  
<sup>24</sup>T. Lorenz, B. Buchner, P. H. M. van Loosdrecht, F. Shonfield, G. Chouteau, A. Revcolevschi, and G. Challenor, *Phys. Rev. Lett.* **81**, 148 (1998).  
<sup>25</sup>R. Blinc, U. Micac, T. Apih, J. Dolinsek, J. Seliger, J. Slak, S. Zumer, L. Guibe, and D. Ailion, *Phys. Rev. Lett.* **88**, 015701 (2002).  
<sup>26</sup>B. Topic, U. Haeberlen, and R. Blinc, *Phys. Rev. B* **42**, 7790 (1990).

- <sup>27</sup>R. Blinc, P. Prelovsek, and R. Kind, *Phys. Rev. B* **27**, 5404 (1983).
- <sup>28</sup>T. Aphih, U. Mikac, J. Dolinsek, J. Seliger, and R. Blinc, *Phys. Rev. B* **61**, 1003 (2000).
- <sup>29</sup>T. Aphih, U. Mikac, J. Seliger, J. Dolinsek, and R. Blinc, *Phys. Rev. Lett.* **80**, 2225 (1998).
- <sup>30</sup>H. Schmid, *Int. J. Magn.* **4**, 337 (1973).
- <sup>31</sup>H. Schmid, *Ferroelectrics* **252**, 41 (2001).
- <sup>32</sup>V. Dubovik, S. Krotov, and V. Tugusheve, *Sov. Phys. Crystallogr.* **32**, 314 (1987).
- <sup>33</sup>E. Ascher, *Magnetolectric Interaction Phenomena in Crystals*, edited by A. Freeman and H. Schmid (Gordon and Breach, New York, 1975), p. 69.
- <sup>34</sup>Yu. M. Sirotnin and M. P. Shaskol'skaya, *The Fundamentals of Crystallography* (Nauka, Moscow, 1975).
- <sup>35</sup>V. Ginsburg, A. Gorbatsevich, Yu. Kopaev, and B. Volkov, *Solid State Commun.* **50**, 339 (1987).
- <sup>36</sup>J. Ohtani and K. Kohn, *J. Phys. Soc. Jpn.* **53**, 3744 (1984).
- <sup>37</sup>R. Birss, *Symmetry and Magnetism* (North-Holland, Amsterdam, 1964).
- <sup>38</sup>C. Tabares-Munoz, J. Rivera, A. Bezinges, A. Monnier, and H. Schmid, *Jpn. J. Appl. Phys., Part 1* **24**, 1051 (1984).
- <sup>39</sup>V. Eremenko, A. V. Klochko, V. M. Naumenko, and V. V. Pishko, *JETP Lett.* **40**, 986 (1984).
- <sup>40</sup>S. A. Zvyagin, J. Krzystek, P. H. M. van Loosdrecht, G. Dhalenne, and A. Revcolevschi, *Phys. Rev. B* **67**, 212403 (2003).
- <sup>41</sup>W. Palme *et al.*, *Phys. Rev. Lett.* **76**, 4817 (1996).
- <sup>42</sup>S. A. Zvyagin (unpublished).
- <sup>43</sup>L. D. Landau and E. M. Lifshitz, *Statistical Physics. Course of Theoretical Physics* (Pergamon, Oxford, 1997), Vol. V.
- <sup>44</sup>M. M. Tehranchi, N. F. Kubrakov, and A. K. Zvezdin, *Ferroelectrics* **204**, 181 (1997).
- <sup>45</sup>A. K. Zvezdin and A. Mukhim, *JETP* **102**, 577 (1992).
- <sup>46</sup>See EPAPS Document No. E-PRBMDO-69-019406 for supplementary material on the Landau-Ginzburg formalism. A direct link to this document may be found in the online article's HTML reference section. The document may also be reached via the EPAPS homepage (<http://www.aip.org/pubservs/epaps.html>) or from <ftp.aip.org> in the directory /epaps/. See the EPAPS homepage for more information.
- <sup>47</sup>Z. V. Gabbasova, M. D. Kuz'min, A. K. Zvezdin, L. S. Dubenko, V. A. Murashov, D. N. Rakov, and I. B. Krynetsky, *Phys. Lett. A* **158**, 491 (1991).